Talanta 114 (2013) 5–10

Contents lists available at ScienceDirect

Talanta

journal homepage: www.elsevier.com/locate/talanta

A facile label-free electrochemiluminescence biosensor for target protein specific recognition based on the controlled-release delivery system

Xiaoyan Yang *, Aiguo Wang, Jilong Liu

Shandong Provincial Key Laboratory of Biochemical Analysis, College of Chemistry and Molecular Engineering, Qingdao University of Science and Technology, Qingdao 266042, Shandong, PR China

ARTICLE INFO

Article history:
Received 3 January 2013
Received in revised form
17 March 2013
Accepted 28 March 2013
Available online 6 April 2013

Keywords:
Electrochemiluminescence
Label-free
Controlled-delivery
Iron oxide
Mesoporous silica

ABSTRACT

This paper described a novel label-free electrochemiluminescence assay for target protein based on a controlled delivery system. Iron oxide magnetic mesoporous silica nanocontainers were prepared by using a general procedure. The prepared magnetic mesoporous silica nanocontainers were applied to load the guest molecules $[Ru(bpy)_3]^{2+}$. Aptamers were used as gatekeepers on the pore outlets of the nanocontainers. In the presence of target proteins, the specific aptamer–protein interactions were employed as triggers for uncapping the pores and releasing the guest molecules from the nanocontainers. The amount of the guest molecule $[Ru(bpy)_3]^{2+}$ released from the magnetic mesoporous silica nanocontainers was monitored by the electrochemiluminescence assay. The results show that the releasing amount of $[Ru(bpy)_3]^{2+}$ is proportional to the thrombin concentration in the range of 0.6 pM–0.8 nM with a detection limit of 0.5 pM ($S/N=3$). The present work demonstrates that the fabricated nanocontainer using aptamer as the cap is a highly sensitive and selective key-in lock gating system for the label-free ECL biosensor.

1. Introduction

Electrochemiluminescence (ECL) has been a very powerful analytical technique which is widely used in the areas of clinical tests and biomolecule detection [1]. $[Ru(bpy)_3]^{2+}$ is a well-known ECL luminophore with high ECL efficiency, which is often used to label DNA, antibody or antigen in ECL biosensor [2–5]. In order to tag biomolecule, it is necessary to functionalize $[Ru(bpy)_3]^{2+}$ with active group, such as –COOH, $–NH_2$, –SH, etc, resulting in the complicated and time-consuming labeling process. Compared with the conventional label-based methods, label-free ECL biosensors have attracted much attention in recent years owing to avoiding the need for expensive and complex molecular labels [6–12]. However, most of label-free ECL biosensors were "signal-off" architectures, in which the presence of targets could reduce ECL intensity and sensitivity. Therefore, developing a signal-on, low-cost and efficient approach is the key issue to improve the ECL label-free biosensor.

Magnetic mesoporous silica nanocontainers (MMSNs) have gained increasing attention for their interesting magnetic property, large surface area, accessible pore volume, and well-defined surface property. MMSNs have provided an alternative for site-specific drug targeting delivery because they could be concentrated and held in position by means of an external field [13]. Furthermore, they could be used in bioseparation of protein or cell, and diagnosis as potential contrast agents in magnetic resonance imaging [14]. There have been some reports on the preparation of magnetic iron nanoparticles coated with mesoporous shells [15–19]. And there have been several reports on the controlled-release of the cargos based on the magnetic mesoporous silica nanoparticles for drug delivery, simultaneous magnetic resonance and fluorescence imaging [15–20]. However, to the best of our knowledge, the label-free ECL biosensors with signal-on architecture based on a controlled-release MMSNs system has not been reported yet.

Herein, we described a general procedure for the fabrication of Fe_3O_4 magnetic nanoparticles embedded within mesoporous silica nanocontainers. Furthermore, these monodisperse MMSNs were applied to the uptake and controlled release of guest molecules by using aptamers as gatekeepers. Aptamers are the short single-stranded nucleic acids which bind to their respective target molecules with high affinity and specificity [21–24]. As excellent alternatives to antibodies, aptamers have been used in molecule recognition and detection as well as targeted drug-delivery systems [25–28]. In this work, the specific aptamer–protein interactions were employed as triggers for uncapping the pores and releasing the guest molecules from MMSNs. Thrombin, a multifunctional serine protease involves in the coagulation cascade and converts fibrinogen to insoluble fibrin that forms the fibrin gel, was chosen as the target protein model [29]. Accordingly, the aptamer of thrombin was chosen as the gatekeeper. $[Ru(bpy)_3]^{2+}$,

* Corresponding author. Tel.: +86 532 84022750; fax: +86 532 84023927.
E-mail address: yangxiaoyan_zh@126.com.(X. Yang)

0039-9140/$ - see front matter Crown Copyright © 2013 Published by Elsevier B.V. All rights reserved.
http://dx.doi.org/10.1016/j.talanta.2013.03.077

a typical ECL substrate, was employed as the guest molecule to be encapsulated within the MMSNs. This flexible ECL biosensor exhibited not only high sensitivity and specificity but also excellent performance in real human plasma samples.

2. Experimental

2.1. Reagents and apparatus

Tetraethylorthosilicate (TEOS), n-cetyltrimethylammonium bromide (CTAB) and oleic acid were purchased from Bodi Chemical Co., Ltd. (Tianjin, China). Iron (III) chloride hexahydrate ($FeCl_3 \cdot 6H_2O$), iron (II) chloride tetrahydrate ($FeCl_2 \cdot 4H_2O$) and cerium(III) nitrate hexahydrate ($Ce(NO_3)_3 \cdot 6H_2O$) were obtained from DaMao Chemical Reagent Factory (Tianjin, China). 3-Aminopropyltriethoxysilane (APTS), and Tris(2,2′-bipyridyl)ruthenium(II) chloride hexahydrate ($[Ru(bpy)_3]Cl_2 \cdot 6H_2O$) were purchased from J&K Chemical LTD. (Beijing, China). Purified thrombin (1000 U/mg, lyophilized powder) was purchased from Dingguo biological Technology Corporation (Beijing, China). Lysozyme, trypsin and bovine serum albumin (BSA) were purchased from Sigma (USA). Analytical reagent grade chemicals and deionized, doubly distilled water (18.2 MΩ cm) were used throughout.

The compositions of the buffer solutions used for the experiments were as follows: buffer solution for washing and for the immobilization of the aptamer onto NH_2–MSN was 20 mM Tris–HCl solution, for the interaction between aptamer and thrombin physiological buffer was PBS solution (0.1 M NaH_2PO_4–Na_2HPO_4, pH=7.0, containing 10 mM KCl, 2 mM $MgCl_2$), and the solution for ECL detection consisted of Britton–Robinson buffer (B–R buffer, 0.04 M H_3BO_3, 0.04 M H_3PO_4, and 0.04 M CH_3COOH, pH=8.69), 0.1 M potassium persulfate, and 2.0 M NaCl.

Oligonucleotides were synthesized by SBS-bio Genetech. Co. Ltd. (Shanghai, China). Their base sequences were as follows:

Aptamer : 5′–TTT TTT GGT TGG TGT GGT TGG–3′.

Transmission electron microscopy (TEM), Zeta Potential, Dynamic Light Scattering (DLS), XRD microscopy, Vibrating Sample Magnetometer (VSM) and N_2 adsorption–desorption were employed to characterize the synthesized materials. TEM image was taken with a JEOL JEM-2100 instrument (HITACHI). Zeta Potential and DLS were performed on a Malvern Zetasizer-Nano instrument equipped with a 4 mW He–Ne laser (633 nm) and avalanche photodiode detector. X-ray measurements were performed on a D/max2500PC diffractometer (RIGAKU) using Cu-Kα radiation. N_2 adsorption–desorption isotherms were recorded on a Micromeritics Tristar 3000 analyzer. The samples were degassed at 120 °C in vacuum overnight. The specific surface areas were calculated from the adsorption data in the low pressures range using the Barrett–Emmett–Teller (BET) model. Pore volume and pore size distributions for the adsorption branch of the isotherm were determined following the Barrett–Joyner–Halanda (BJH) method. UV–vis spectra were carried out on a Cary 50 UV–vis–NIR spectrophotometer (Varian).

2.2. Preparation of Fe_3O_4 nanoparticles

The magnetic nanoparticles were prepared via a convenient chemical coprecipitation process described previously with a slight modification [17]. Briefly, 4.80 g $FeCl_3 \cdot 6H_2O$ and 2.00 g $FeCl_2 \cdot 4H_2O$ were added to 120 mL of deionized water under nitrogen atmosphere with vigorous stirring. 20 mL of ammonium hydroxide (14 wt%) was then added to the mixture solution at 70 °C and kept for 30 min. 0.85 mL oleic acid was added and the reaction was kept for another 2.5 h at 70 °C. The black precipitate was collected by magnetic separation at room temperature, washed with ethanol 3 times by ultrasonication for 5 min, collected by centrifugation at 10,000 r/min, and kept wet at 4 °C for use.

2.3. Synthesis of magnetic mesoporous silica nanocontainers (MMSNs)

The MMSNs were prepared according to the method reported previously with a slight modification [17–19]. 0.15 g as-prepared Fe_3O_4 nanoparticles were dispersed in 20 mL of aqueous solution containing 0.40 g of CTAB with vigorous stirring. Then 20 mL of the as-synthesized aqueous phase monodisperse Fe_3O_4 nanoparticles was added into the 172 mL of aqueous solution containing 0.10 g of CTAB and 1.4 mL of NaOH (2.0 M) with vigorous stirring, and the mixed solution was heated to 75 °C and 2.5 mL of TEOS was introduced under vigorous stirring. After 15 min of stirring, 100 μL of APTS was added into the mixtures, and the solution was stirred for 2 h. The light brown product was collected by filtration and dried at room temperature. The CTAB surfactants were removed from the mesopores by dispersing the as-synthesized materials in a solution of 0.160 g of ammonium nitrate and 60 mL of 95% ethanol and heating the mixture at 60 °C for 15 min to fabricate the NH_2-group functionalized MMSNs (NH_2–MMSNs).

2.4. Preparation of dye encapsulated NH_2–MMSNs

0.1 g the above NH_2–MMSNs solid and the dye tris (2,2′-bipyridyl) ruthenium chloride (0.06 g, 0.08 mmol) were suspended in 2 mL of anhydrous acetonitrile under N_2 atmosphere. The suspension was stirred for 24 h at room temperature with the aim of encapsulating dye into the pores of the MMSN scaffolding. The solution was dried in vacuum to remove acetonitrile, and then the obtained orange solid was suspended in 2 mL Tris–HCl (20 mM) buffer.

2.5. Fabrication of the aptamer as the cap of the controlled-release system

20 μL aptamer solutions were added into 5 μL NH_2–MMSNs loaded with guest dyes suspension, incubated for 30 min at 37 °C with frequent shaking. The resulting solid was isolated by magnetic separation and washed 3 times with Tris–HCl buffer to remove the residual dye and the free aptamer.

2.6. Release of the guest molecules

20 μL thrombin solutions were added in the above aptamer-capped NH_2–MMSNs solid loaded with guest molecules, incubated at 37 °C for 2 h. Supernatant containing the guest molecules released from MMSNs was obtained after magnetic separation. The release efficiency of the guest molecules was determined by UV–vis spectra at a wavelength of 286 nm, using an extinction coefficient of 7.95×10^4 L mol^{-1} cm^{-1}.

2.7. ECL detection

The ECL emission was detected by the use of a model MPI-E ECL analyzer (Xi'an Remax Electronic Science & Technology Co. Ltd., Xi'an, China) at room temperature. A commercial cylindroid glass cell with three-electrode, a 2.5-mm diameter Au as the working electrode, a Pt wire as the counter electrode, and an Ag/AgCl (sat.) as the reference electrode, was used. 20 μL supernatant containing the guest molecules released from MMSNs, 800 μL detection solution (B–R buffer solution, 0.1 M potassium persulfate, and 2.0 M NaCl), and 180 μL 1.0 mM cerium nitrate solution were added in a quartz cell for ECL detection. Cyclic voltammetry mode with continuously potential scanning from −1.9 to 0.0 V and with 350 mV s^{-1} scanning rate

was applied to achieve ECL signal. A high voltage of −500 V was supplied to the photomultiplier for determining the luminescence intensity. The ECL and CV curves were recorded simultaneously.

2.8. Plasma samples and in situ generation of thrombin

Pretreatment plasma was activated by using 0.25% trypsin (containing 1 mM Ca^{2+}) and 5.3×10^{-3} M the fish DNA, and then was diluted 10, 100, 1000 times. The following experiments were same as that of the standard thrombin solution.

3. Results and discussion

3.1. Mechanism of the controlled-release system

The novel label-free ECL biosensor for thrombin assay based on the controlled-release MMSNs system was successfully designed. The fabrication principle of the strategy was shown in Fig. 1. The NH_2-group functionalized MMSNs (NH_2–MMSNs) was fabricated first. $[Ru(bpy)_3]^{2+}$ as the guest molecule was encapsulated into the pores of the NH_2–MMSNs. A 15-mer thrombin-binding aptamer, one of the most intensively studied ss-DNA which bound to thrombin with a dissociation constant of 25 nM, was chosen as a gatekeeper [30]. In the absence of thrombin target molecule, the aptamer was naturally unfolded. The unfolded aptamer was absorbed on NH_2–MMSN through electrostatic interaction between the positively charged NH_2–MMSN (ζ-potential = 13.1 mV) and the negatively charged ss-DNA, resulting in the capping of the pores. The successful introduction of NH_2-group, aptamer at various stages of loading and release was confirmed in detail by zeta potential measurements (Table S1, See the Supporting material). In the presence of thrombin, the interaction of aptamer with thrombin changed the conformation into G-quadruplex form, and then the aptamer displaced from the surface of MMSN [26,28], resulting in uncapping the pores and releasing the guest molecules. Supernatant containing the guest molecules released from MMSNs was obtained after magnetic separation, which could be easily detected and quantified by electrochemiluminescence (ECL) assay. In this work, we used a typical reductive-oxidation ECL system, $[Ru(bpy)_3]^{2+}$–$S_2O_8^{2-}$ to monitor the release of $[Ru(bpy)_3]^{2+}$ from the MMSNs after magnetic separation of the solid MMSNs. Ce^{3+} was applied as a signal enhancer in this system to obtain continuous and stable ECL signal [31].

3.2. Preparation and characterization of magnetic mesoporous silica nanocontainers

As shown in Fig. 2, uniform MMSNs were prepared via a modified approach as described previously [17–19]. Firstly, magnetic nanoparticles were prepared using a convenient chemical coprecipitation process reported previously with a slight modification and stabilized with hydrophilic oleic acid [17]. In order to prepare water-dispersible nanoparticles, CTAB was employed as the stabilizing secondary surfactant for the transfer of the iron nanoparticles suspension from organic phase to aqueous phase [15]. The subsequent sol–gel reaction of the silica precursor TEOS in an aqueous solution containing CTAB and oleic acid-stabilized magnetite nanoparticles suspension generated MMSNs following by removal of the organic templates CTAB.

The as-synthesized Fe_3O_4 nanoparticles have an average diameter of 25 nm estimated from the transmission electron microscopy (TEM) images (See the Supporting material, Fig. S1). The TEM images (Fig. 2, left) of MMSNs show that the MMSNs are quite uniform in size with an average diameter of 100 nm. It can be seen that each silica sphere contains one monodisperse magnetite nanoparticle and possesses a well-ordered mesoporous structure. The photographs indicate that the magnetic mesoporous silica spheres in the buffer solution possess the superparamagnetic character desirable for their applications to separation and delivery (Fig. 2, middle and right). Magnetic characterization at 300 K shows that the magnetization saturation value of Fe_3O_4 and MMSN nanoparticles is 60.0 and 5.6 emu g^{-1}, respectively (Fig. 3a). It can be seen that both the MMSN nanoparticles and Fe_3O_4 show ferromagnetic behavior, and the saturation magnetization (*Ms*) values are sufficient to allow them to be separated easily from the solution with the help of external magnet force. Compared to the traditional separation procedures, magnetic separation technique is very simple, and all steps of the purification can take place in one tube under a magnetic field [32]. Therefore, we have used magnetic separation technique during the following processes of the capping, releasing the guest molecules. The decrease in magnetic saturation for MMSN nanoparticles can be explained by taking into account the diamagnetic contribution of the silica sphere surrounding the magnetic Fe_3O_4 cores. In Fig. 3b, the broadband centered at $2\theta = 22^\circ$ can be assigned to the characteristic reflection from amorphous SiO_2. Wide-angle XRD patters show that the diffraction peaks of the MMSNs are similar to the sharpened spinel (220), (311) and (440) peaks of Fe_3O_4 suggesting that the Fe_3O_4 nanocrystals are well incorporated into the silica matrix and still

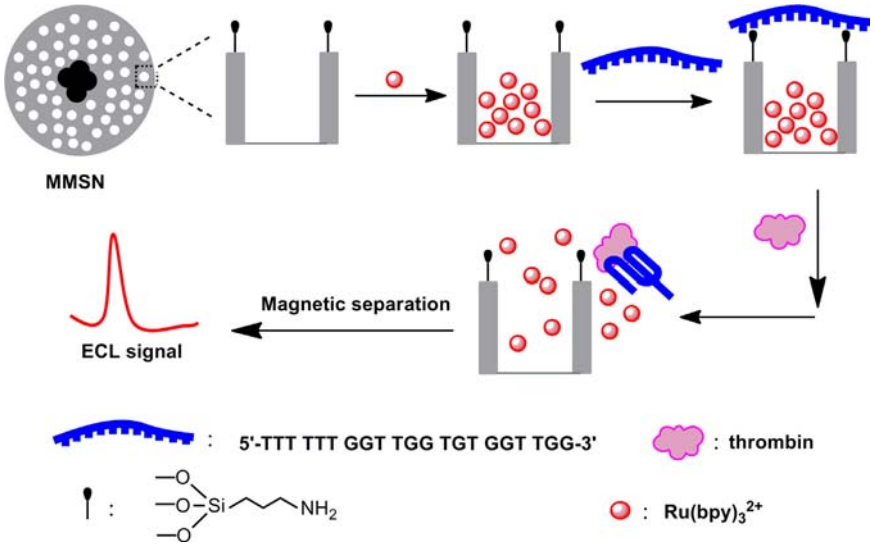

Fig. 1. Schematic representation of the thrombin-bioreponsive MMSN based delivery system as the label-free electrochemiluminescence platform.

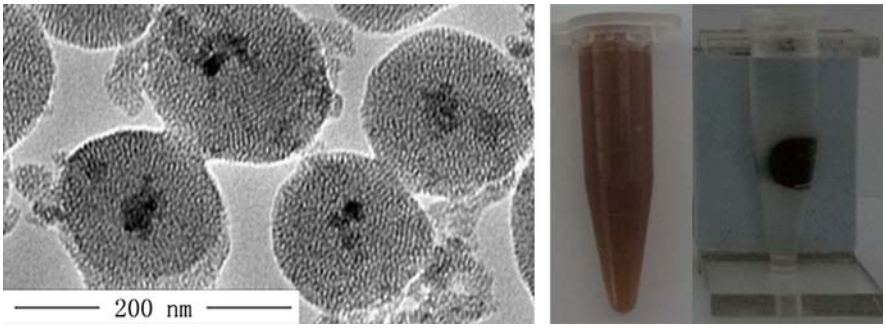

Fig. 2. TEM micrographs of MMSN (left), and photographs of MMSN suspension in the absence (middle) and in the presence of a magnet (right).

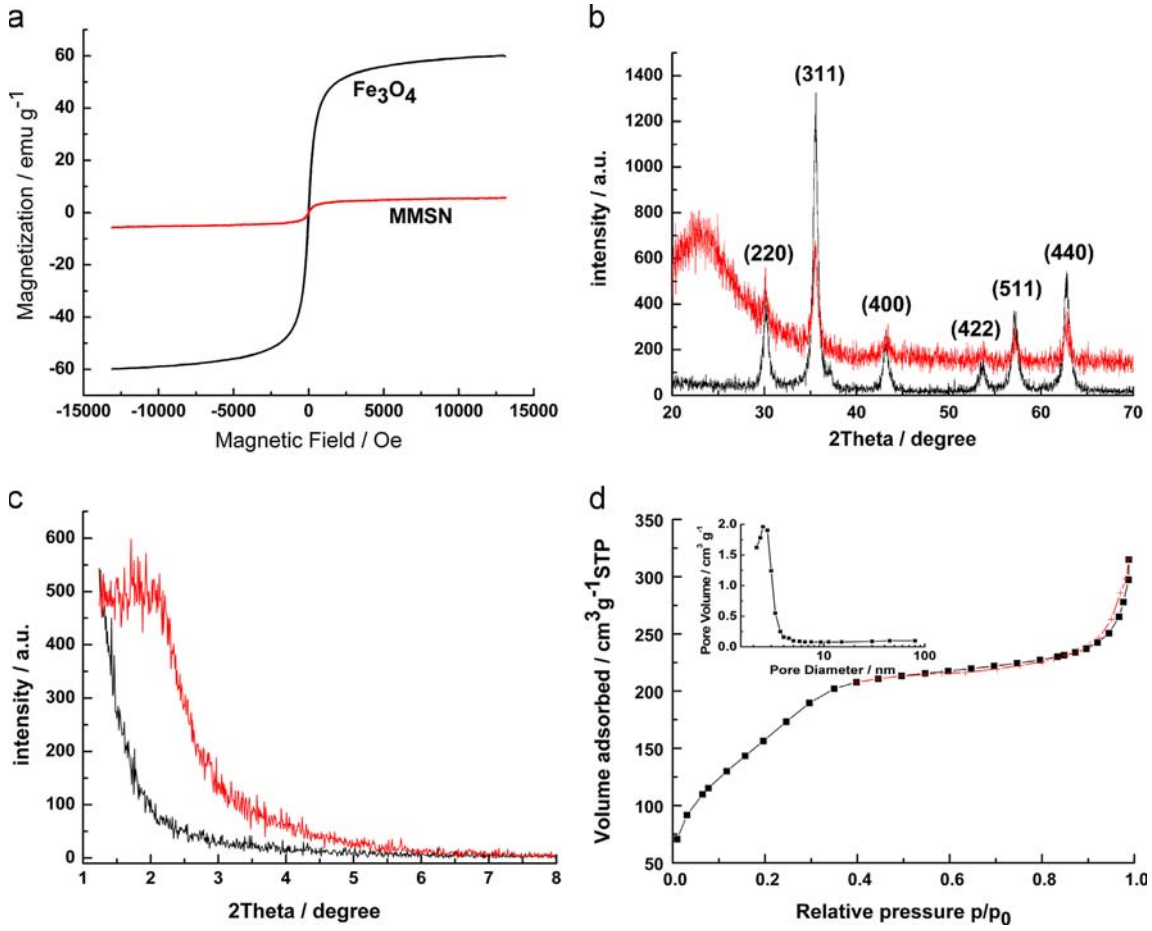

Fig. 3. (a) The magnetic hysteresis loops of MMSN (red line), Fe_3O_4 nanoparticles (black line); (b) Powder X-ray diffraction patterns of MMSN (red line), Fe_3O_4 nanoparticles (black line); (c) Low-angle powder X-ray diffraction patters of MMSN (red line), Fe_3O_4 nanoparticles (black line); (d) Nitrogen adsorption/desorption isotherms and BJH pore size distributions from adsorption branch (insert) of MMSN. (For interpretation of the references to color in this figure legend, the reader is referred to the web version of this article.)

retain their magnetite crystalline structure. The low-angle XRD shows that the MMSN has hexagonal mesopore symmetry (Fig. 3c). The pore size was calculated using the BJH method to be 3.5 nm (Fig. 3d, inset). The BET surface area and the total pore volume were 598 $m^2\ g^{-1}$ and 0.56 $cm^3\ g^{-1}$, respectively. The corresponding N_2 adsorption/desorption isotherms were shown in Fig. 3d.

3.3. The optimization for the preparation of aptamer to cap NH_2–MMSN

The optimization for the preparation of aptamer to cap NH_2–MMSN was carried out by measuring the ECL intensity of the released guests after uncapping the pores. The capping processes were performed in the presence of different amounts of aptamer, and the subsequent controlled releasing processes were characterized by using 10 nM thrombin solution. The ECL intensity of the released $[Ru(bpy)_3]^{2+}$ in the different solutions were measured. As shown in Fig. S2, 10 nM aptamer was the optimal concentration to cap all the mesopores of MMSN.

3.4. Controlled release of guest molecules from MMSN

To investigate the gating properties, the release behavior as a function of time in the presence and absence of thrombin was displayed in Fig. 4. The results show that MMSNs inorganic supports display clear delivery of guest molecules in the presence of 10 nM

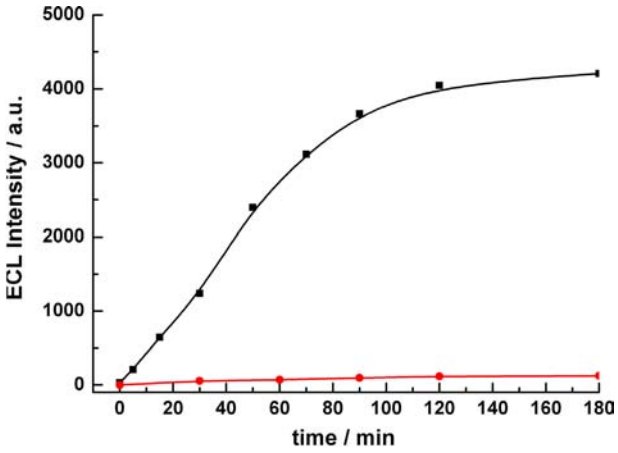

Fig. 4. Release profiles of $[Ru(bpy)_3]^{2+}$ guest molecules monitored by the following ECL intensity in B–R suspensions after magnetic separation of the capped solid MMSN in the absence (red line) and in the presence (blank line) of thrombin, the concentration of thrombin is 10 nM. (For interpretation of the references to color in this figure legend, the reader is referred to the web version of this article.)

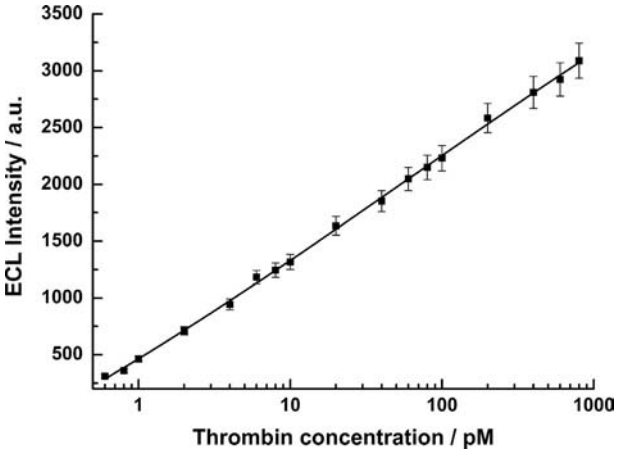

Fig. 5. Controlled release of $[Ru(bpy)_3]^{2+}$ from the MMSN capped with aptamers triggered by thrombin as a function of concentration. Error bars are standard deviation of three repetitive measurements.

thrombin (Fig. 4, blank curve). And 85% of the maximum release of the encapsulated cargos was observed after 2 h. However, MMSNs supports display negligible delivery of guest molecules in the absence of thrombin even after 3 h (Fig. 4, red curve), indicating a good capping efficiency of the aptamer.

Delivery from MMSNs as a function of the concentration of the molecular trigger thrombin was studied. As shown in Fig. 5, it can be seen that the release of $[Ru(bpy)_3]^{2+}$ strongly depends on the concentration of thrombin, ECL intensity increases with the increase of thrombin concentration and exhibits a linear correlation with thrombin concentration over a range of 3 orders of magnitude from 0.6 pM to 0.8 nM. The linear regression equation is $\Delta I = 899.27 \log_{10}C + 452.03$ (ΔI is the ECL intensity subtracted the blank and C was the concentration of thrombin), with a correlation coefficient of 0.9994. A detection limit of 0.5 pM was achieved ($S/N=3$). And the relative standard deviation (RSD) was calculated to be 4.9% ($n=7$) for the detection of 2.0 pM thrombin, indicating that the precision and reproducibility of the proposed method are acceptable.

3.5. Selectivity of the delivery system

To investigate the selectivity of the delivery system, guest delivery by MMSNs was tested separately in the presence of 1.0 μM other proteins, such as bovine serum albumin (BSA), lysozyme, and glucose oxidase (GOD). The results were compared with those obtained from the analyses of 0.1 nM thrombin. The uncapping ability of these proteins was shown in Fig. 6, it could be found that only the thrombin sample showed a maximal relative ECL intensity, while the other three proteins had almost negligible relative ECL intensity. The cross-sensitivity of the proposed method in a mixture of four different proteins containing thrombin was also examined. The signal obtained from the complex was similar to that obtained from only thrombin, indicating that BSA, lysozyme and GOD had almost negligible uncapping ability.

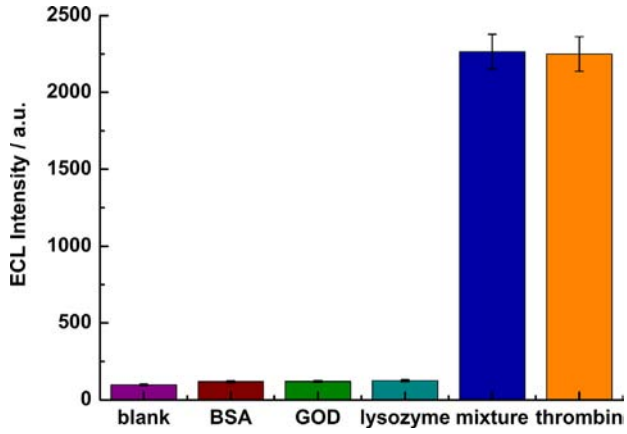

Fig. 6. Selective release profiles for aptamer–protein responsive controlled delivery system triggered by BSA, lysozyme, GOD, and the mixture of BSA, lysozyme, GOD and thrombin, respectively.

3.6. Controlled release of guest molecules from MMSN in human plasma samples

Thrombin is not present in blood and plasma of healthy subjects when coagulation is not occurring. Prothrombin, the precursor of thrombin, is present in plasma and can be converted to thrombin via a proteolytic process by activated factor X [22,24]. In this work, the generation of thrombin was performed according to the references [22,24], and the release profiles of $[Ru(bpy)_3]^{2+}$ guest molecules in the healthy human plasma detected by the proposed assay were shown in Fig. S3. The relative ECL intensity exhibited a linear correlation with the diluted times of the plasma sample. The results suggested that the proposed system could be applied for the drug delivery in the presence of the target biomolecules.

4. Conclusion

In this study, an universal approach to fabricating signal-on ECL aptasensors was proposed. The MMSNs were applied to the load of guest molecules $[Ru(bpy)_3]^{2+}$ and the aptamers were used as the gatekeepers. The specific aptamer–protein interactions were employed as triggers for uncapping the pores and releasing the guest molecules from MMSNs. Using this controlled-release system, we detected the thrombin with a detection limit of 0.8 pM. Compared with the existing ECL aptamer biosensors, the proposed ECL detection strategy is simple, low-cost, and highly selective. Moreover, the as-synthesized MMSN could be used as not only the nanocontainer for the load of guest molecules but also as the convenient separating platform under the magnetic field. The MMSNs offer new opportunities for accurate timing controlled and in vivo site-specific drug delivery of biomedical applications. And such ECL aptasensor provides new possibilities for protein diagnostics as well as for bioanalysis in general.

Acknowledgments

This research was supported by the National Nature Science Foundation of China (Nos. 21005044 and 21025523), Excellent Young Scientists Encouragement Foundation of Shandong Province (BS2011CL017), and the Nature Science Foundation of Shandong Province (ZR2012BM011).

Appendix A. Supporting information

Supplementary data associated with this article can be found in the online version at http://dx.doi.org/10.1016/j.talanta.2013.03.077.

References

[1] W. Miao, Chem. Rev. 108 (2008) 2506–2553.
[2] Y. Li, H. Qi, Y. Peng, J. Yang, C. Zhang, Electrochem. Commun. 9 (2007) 2571–2575.
[3] X.H. Xu, R.B. Jeffers, J. Gao, B. Logan, Analyst 126 (2001) 1285–1292.
[4] W. Miao, A.J. Bard, Anal. Chem. 75 (2003) 5825–5834.
[5] W. Yao, L. Wang, H. Wang, X. Zhang, L. Li, Biosens. Bioelectron. 24 (2009) 3269–3274.
[6] G. Jie, H. Huang, X. Sun, J. Zhu, Biosens. Bioelectron. 23 (2008) 1896–1899.
[7] G. Jie, B. Liu, H. Pan, J. Zhu, H.Y. Chen, Anal. Chem. 79 (2007) 5574–5581.
[8] X.B. Yin, Y.Y. Xin, Y. Zhao, Anal. Chem. 81 (2009) 9299–9305.
[9] L. Hu, Z. Bian, H. Li, S. Han, Y. Yuan, L. Gao, G. Xu, Anal. Chem. 81 (2009) 9807–9811.
[10] T. Yuan, Z. Liu, L. Hu, L. Zhang, G. Xu, Chem. Commun. 47 (2011) 11951–11953.
[11] E. Han, L. Ding, S. Jin, H. Ju, Biosens. Bioelectron. 26 (2011) 2500–2505.
[12] D. Liu, Y. Xin, X. He, X. Yin, Biosens. Bioelectron. 26 (2011) 2703–2706.
[13] A.S. Lübbe, C. Bergemann, J. Brock, D.G. McClure, J. Magn. Magn. Mater. 194 (1999) 149–155.
[14] M. Mahmoudi, H. Hosseinkhani, M. Hosseinkhani, S. Boutry, A. Simchi, W. S. Journeay, K. Subramani, S. Laurent, Chem. Rev. 111 (2011) 253–280.
[15] J. Kim, J.E. Lee, J. Lee, J.H. Yu, B.C. Kim, K. An, Y. Hwang, C.H. Shin, J.G. Park, J. Am. Chem. Soc. 128 (2006) 688–689.
[16] Y. Deng, D. Qi, C. Deng, X. Zhang, D. Zhao, J. Am. Chem. Soc. 130 (2008) 28–29.
[17] Y. Lin, C.L. Haynes, Chem. Mater. 21 (2009) 3979–3986.
[18] L. Zhang, S. Qiao, Y. Jin, H. Yang, S. Budihartono, F. Stahr, Z. Yan, X. Wang, Z. Hao, G.Q. Lu, Adv. Funct. Mater. 18 (2008) 3203–3212.
[19] S. Febvay, D.M. Marini, A.M. Belcher, D.E. Clapham, Nano Lett. 10 (2010) 2211–2219.
[20] C.R. Thomas, D.P. Ferris, J.H. Lee, E. Choi, M.H. Cho, E.S. Kim, J.F. Stoddart, J.S. Shin, J. Cheon, J.I. Zink, J. Am. Chem. Soc. 132 (2010) 10623–10625.
[21] X. Li, J. Liu, S. Zhang, Chem. Commun. 46 (2010) 595–597.
[22] S. Centi, S. Tombelli, M. Minunni, M. Mascini, Anal. Chem. 79 (2007) 1466–1473.
[23] C. Ding, Y. Ge, S. Zhang, Chem.-Euro. J 16 (2010) 10707–10714.
[24] G.A. Zelada, S.V. Bhosale, J. Riu, F.X. Rius, Anal. Chem. 82 (2010) 9254–9260.
[25] Y. Du, B. Li, H. Wei, Y. Wang, E. Wang, Anal. Chem. 80 (2008) 5110–5117.
[26] A. Heckel, G. Mayer, J. Am. Chem. Soc. 127 (2005) 822–823.
[27] Z. Cao, R. Tong, A. Mishra, W. Xu, G.C.L. Wong, J. Cheng, Y. Lu, Angew. Chem. Int. Ed. 48 (2009) 6494–6498.
[28] J. Zheng, G.F. Cheng, P.G. He, Y.Z. Fang, Talanta 80 (2010) 1868–1872.
[29] M.P.A. Ebert, S. Lamer, J. Meuer, P. Malfertheiner, M. Reymond, T. Buschmann, C. Röcken, V. Seibert, J. Proteome Res 4 (2005) 586–590.
[30] H. Cho, B.R. Baker, S. Wachsmann-Hogiu, C.V. Pagba, T.A. Laurence, S.M. Lane, L.P. Lee, J.B.H. Tok, Nano Lett. 8 (2008) 4386–4390.
[31] A.W. Knight, G.M. Greenway, Analyst 120 (1995) 2543–2547.
[32] S. Laurent, D. Forge, M. Port, A. Roch, C. Robic, L. Vander Elst, R.N. Muller, Chem. Rev. 108 (2008) 2064–2110.